New Journal of Physics
The open access journal at the forefront of physics

Deutsche Physikalische Gesellschaft DPG
IOP Institute of Physics

Published in partnership with: Deutsche Physikalische Gesellschaft and the Institute of Physics

OPEN ACCESS

RECEIVED
15 September 2014

REVISED
7 February 2015

ACCEPTED FOR PUBLICATION
10 February 2015

PUBLISHED
12 March 2015

PAPER

Instability of a thin conducting foil accelerated by a finite wavelength intense laser

B Eliasson

SUPA, Physics Department, John Anderson Building, Strathclyde University, Glasgow G4 0NG, Scotland, UK

E-mail: bengt.eliasson@strath.ac.uk

Keywords: Rayleigh–Taylor instability, radiation pressure acceleration, thin foil

Abstract

We derive a theoretical model for the Rayleigh–Taylor (RT)-like instability for a thin foil accelerated by an intense laser, taking into account finite-wavelength effects in the laser wave field. These finite-wavelength effects lead to the diffraction of the electromagnetic wave off the periodic structures arising from the instability of the foil, which significantly modifies the growth rate of the RT-like instability when the perturbations on the foil have wavenumbers comparable to or larger than the laser wavenumber. In particular, the growth rate has a local maximum at a perturbation wavenumber approximately equal to the laser wavenumber. The standard RT instability, arising from a pressure difference between the two sides of a foil, is approximately recovered for perturbation wavenumbers smaller than the laser wavenumber. Differences in the results for circular and linear polarization of the laser light are pointed out. The model has significance for radiation pressure acceleration of thin foils, where RT-like instabilities are significant obstacles.

1. Introduction

The Rayleigh–Taylor (RT) instability, or RT-like instabilities [1], is one of the main obstacles preventing greater success of the radiation pressure acceleration scheme in accelerating thin foils of ions by intense lasers [2–8] and hindering the achievement of inertial confinement fusion via laser compression of fuel pellets [9]. For thin foils, it was suggested that the use of a properly tailored laser pulse with a sharp intensity rise [2] or super-Gaussian beams [4, 8] can stabilize the foil, whereas for thicker targets, it was shown that the RT-like instability in the hole-boring radiation pressure acceleration is suppressed by using an elliptically polarized laser [10]. A kinetic theory has also been proposed for a target with distributed electron and ion densities [11]. Although the RT instability was originally associated with a heavier fluid on top of a lighter fluid in a gravitational field [12, 13], similar instabilities occur for plasmas confined by magnetic fields (e.g. [20]) and when a thin foil is accelerated by the pressure difference between the two sides of the foil [1, 2]. The growth rate of the RT instability for laser-accelerated plasma is typically proportional to $\sqrt{gk}$, where g is the acceleration and k the wavenumber of the surface perturbation. This predicts that the instability grows indefinitely for large wavenumbers, whereas in some experiments and simulations, the RT instability gives rise to structures with a spatial periodicity comparable to the laser wavelength [7]. The assumption of a constant normal pressure force is reasonable as long as the perturbations of the foil are relatively small and when the length scales of the perturbations are much larger than the wavelength of the laser [2]. However, laser light has a finite wavelength and is scattered off the periodic structures, leading to a diffraction pattern in the electromagnetic (EM) field. For this case, the 'pressure' picture can be expected to be only approximate for monochromatic laser light. Theoretical investigations of the instabilities resulting from the scattering of EM waves off plasma surface perturbations include the RT instability of an over-dense plasma layer [14] using a magnetohydrodynamic-like model for the plasma, and the scattering off surface plasma waves[15, 16] where the electron dynamics is an important source of the instability. The mode coupling of large-amplitude surface plasma waves is also of general interest in plasma columns [17]. The aim of

this paper is to solve the scattering problem and to derive a model for the instability of an ultra-thin perfectly conducting foil accelerated by the radiation pressure of a finite-wavelength intense laser.

2. Theoretical model

We assume that the laser interacts with a foil where the electron density is much higher than the critical density so that no laser light penetrates the foil. For simplicity, we assume an initially planar foil in the x–y plane, with normal incidence of a plane wave laser light propagating in the positive z-direction. This assumption is reasonable also near the center of a laser pulse with a finite width if the spot is at least a few laser wavelengths wide and the laser pulse contains a significant number of laser periods. In this case, we can carry out a stability analysis based on a Fourier decomposition of the problem in space and time. With smaller spot sizes comparable to the laser wavelength and/or shorter pulses (such as the lambda cubed regime), more advanced methods need to be employed, for example, based on the decomposition of a laser beam in terms of Laguerre–Gaussian modes.

We carry out the calculations in a frame moving with the velocity of the unperturbed foil. In this frame, the dynamics of the initially small-amplitude perturbations of the foil are non-relativistic. The results obtained in the moving frame can later be Lorentz transformed into the laboratory frame, but here we will assume for simplicity that the speed of the foil is non-relativistic. The velocity $\mathbf{v}$ of the foil relative to the accelerated frame is governed by the momentum equation

$$M\left(\frac{\partial}{\partial t}+v_x\frac{\partial}{\partial x}+v_y\frac{\partial}{\partial y}\right)\mathbf{v}=\mathbf{F}-Mg_0\hat{\mathbf{z}}, \tag{1}$$

where $M(x,\ y,\ t)$ is the surface mass density, $g_0=F_0/M_0$ is the acceleration of the unperturbed foil in the z-direction, M_0 is the unperturbed areal mass density of the foil, $F_0=2I_0/c$ is the radiation pressure force, I_0 is the incident laser intensity, and c is the speed of light in a vacuum. The force $\mathbf{F}$ is due to the space- and time-dependent EM field acting on the foil. For an unperturbed foil, with $M=M_0$, the force $\mathbf{F}$ would be exactly canceled by the inertial force $-M_0g_0\hat{\mathbf{z}}$, but due to perturbations in the foil, the forces are not exactly canceled, which leads to the RT-like instability. The mass density is governed by the continuity equation

$$\frac{\partial M}{\partial t}+\frac{\partial\left(Mv_x\right)}{\partial x}+\frac{\partial\left(Mv_y\right)}{\partial y}=0. \tag{2}$$

The foil surface can be parameterized as $S(x,\ y,\ z,\ t)=z-\eta(x,\ y,\ t)=0$, where η is the surface elevation of the foil in the z-direction. The velocity and surface elevation are connected through the kinematic condition

$$\frac{\partial\eta}{\partial t}=\mathbf{v}\cdot\nabla S. \tag{3}$$

Equations (1)–(3) are completed by initial conditions on η and on M and $\mathbf{v}$ at $z=\eta$.

First we notice that the assumption of a constant radiation pressure force F_0 acting perpendicularly to the surface on one side of the foil [1, 2] would lead to $\mathbf{F}=F_0\nabla S$ in equation (1) and to a 'standard' RT instability with the growth rate $\sqrt{g_0k}$. Here we will instead determine $\mathbf{F}$ by taking into account that the electric and magnetic fields $\mathbf{E}$ and $\mathbf{B}$ evolve in time according to Maxwell's equations, obeying boundary conditions at the foil surface as well as radiating boundary conditions far away from the foil. We assume that the foil is perfectly conducting, and therefore the electric field parallel to the surface and the magnetic field perpendicular to the surface are zero in a system (denoted by primed variables) moving with the same velocity as the surface, with the boundary conditions expressed as $\mathbf{E}'\times\nabla S=0$ and $\mathbf{B}'\cdot\nabla S=0$ at $z=\eta$. Assuming non-relativistic velocities in the moving frame, the magnetic and electric fields are Galilei transformed from the system moving with the foil surface (primed variables) to the accelerated frame (unprimed variables) as $\mathbf{E}'=\mathbf{E}+\mathbf{v}\times\mathbf{B}$ and $\mathbf{B}'=\mathbf{B}-\mathbf{v}\times\mathbf{E}/c^2\approx\mathbf{B}$. (The term $-\mathbf{v}\times\mathbf{E}/c^2$ will contribute to the boundary conditions only with terms of order v^2/c^2 compared with unity and is therefore neglected.) This gives [17, 18]

$$\mathbf{B}\cdot\nabla S=0 \tag{4}$$

for the magnetic field, whereas for the electric field we have $0=\mathbf{E}'\times\nabla S=(\mathbf{E}+\mathbf{v}\times\mathbf{B})\times\nabla S=\mathbf{E}\times\nabla S-\mathbf{v}(\mathbf{B}\cdot\nabla S)+\mathbf{B}(\mathbf{v}\cdot\nabla S)$, where $\mathbf{B}\cdot\nabla S=0$ and $\mathbf{v}\cdot\nabla S=\partial\eta/\partial t$, giving

$$\mathbf{E}\times\nabla S+\mathbf{B}\frac{\partial\eta}{\partial t}=0 \tag{5}$$

at $z=\eta$.

The force acting on the surface can be calculated using the EM volume force [19]

$$\mathbf{f} = \nabla \cdot \bar{\bar{\boldsymbol{\sigma}}} - \epsilon_0 \frac{\partial}{\partial t}\mathbf{E} \times \mathbf{B}, \tag{6}$$

where

$$\sigma_{ij} = \epsilon_0\left(E_i E_j - \frac{1}{2}\delta_{ij}E^2\right) + \frac{1}{\mu_0}\left(B_i B_j - \frac{1}{2}\delta_{ij}B^2\right) \tag{7}$$

is the Maxwell stress tensor in component form, δ_{ij} represents the unit tensor, ϵ_0 is the electric permittivity in a vacuum, and $\mu_0 = 1/(\epsilon_0 c^2)$ is the magnetic permeability in a vacuum. Integrating $\mathbf{f}$ from $z = \eta - \varepsilon$ to $\eta + \varepsilon$, assuming that $\mathbf{E}$ and $\mathbf{B}$ are zero for $z > \eta$ and letting $\varepsilon \to 0$, gives the EM area force $\mathbf{F} = -\bar{\bar{\boldsymbol{\sigma}}} \cdot \nabla S - \epsilon_0 \mathbf{E} \times \mathbf{B}\partial\eta/\partial t$, which, using the boundary conditions (4) and (5), simplifies to

$$\mathbf{F} = \frac{1}{2}\left(\frac{B^2}{\mu_0} - \epsilon_0 E^2\right)\nabla S. \tag{8}$$

It should be emphasized that in equation (8), $\mathbf{E}$ and $\mathbf{B}$ are the total electric and magnetic fields at the foil surface, to be determined hereafter.

3. Stability analysis

We here give details of a stability analysis of the theoretical model, resulting in the following dispersion relations (20) and (21) for the RT-like instability for circular and linear polarizations of a laser.

Perturbing and linearizing the system of equations (1)–(3) and (8) around the equilibrium solution $\mathbf{v} = 0$, $\eta = 0$, $M = M_0$, $S = z$, $\mathbf{E} = \mathbf{E}_0(t)$, and $\mathbf{B} = \mathbf{B}_0(t)$, gives

$$\frac{\partial^4\eta_1}{\partial t^4} + \frac{F_0^2}{M_0^2}\left(\frac{\partial^2\eta_1}{\partial x^2} + \frac{\partial^2\eta_1}{\partial y^2}\right) = \frac{1}{M_0}\frac{\partial^2}{\partial t^2}\left(\frac{\mathbf{B}_0 \cdot \mathbf{B}_1}{\mu_0} - \epsilon_0 \mathbf{E}_0 \cdot \mathbf{E}_1\right), \tag{9}$$

where the subscript 1 denotes small-amplitude first-order perturbations. For circularly polarized light, the zeroth-order EM force is

$$F_0 = \frac{1}{2}\left(\frac{B_0^2}{\mu_0} - \epsilon_0 E_0^2\right), \tag{10}$$

whereas for linearly polarized light a time averaging over one laser period removes second harmonics and reduces F_0 by a factor of 2 for the given amplitudes B_0 and E_0. Equation (9) is completed by finding the dependence of $\mathbf{E}_1$ and $\mathbf{B}_1$ on η_1. The general form of equation (9) is that of a mode-coupling equation, where the low-frequency perturbations of the foil are driven by the coupling (beating) between the large-amplitude EM wave ($\mathbf{B}_0, \mathbf{E}_0$) and its small-amplitude sidebands ($\mathbf{B}_1, \mathbf{E}_1$).

Writing out the components of the boundary conditions (4) and (5) gives

$$B_z - B_x\frac{\partial\eta}{\partial x} - B_y\frac{\partial\eta}{\partial y} = 0, \tag{11}$$

$$E_y + E_z\frac{\partial\eta}{\partial y} + B_x\frac{\partial\eta}{\partial t} = 0, \tag{12}$$

and

$$E_x + E_z\frac{\partial\eta}{\partial x} - B_y\frac{\partial\eta}{\partial t} = 0, \tag{13}$$

at $z = \eta$. An incident EM wave will be reflected by the foil, and perturbations in the foil surface will lead to the refraction of the wave. The electric and magnetic fields can be written $\mathbf{E} = \mathbf{E}_{i0} + \mathbf{E}_r$ and $\mathbf{B} = \mathbf{B}_{i0} + \mathbf{B}_r$, where $\mathbf{E}_{i0}$ and $\mathbf{B}_{i0}$ are the fields of the incident wave and $\mathbf{E}_r$ and $\mathbf{B}_r$ fields of the reflected wave. In what follows, we show details of the calculations for a circularly polarized incident wave and at the end state only the final result for a linearly polarized wave. More details of the derivations will be given elsewhere. For an incident right-hand circularly polarized EM wave propagating in the z-direction, we have

$$\mathbf{E}_{i0} = \frac{\hat{\mathbf{e}}}{2}\widehat{E}_{i0}\mathrm{e}^{\mathrm{i}\theta_i} + \text{c.c.} \tag{14}$$

and

$$\mathbf{B}_{i0} = \frac{\hat{\mathbf{e}}}{2}\widehat{B}_{i0}\mathrm{e}^{\mathrm{i}\theta_i} + \text{c.c.}, \tag{15}$$

where $\hat{\mathbf{e}} = \hat{\mathbf{x}} + i\hat{\mathbf{y}}$ describes the polarization, $\hat{\mathbf{x}}$ and $\hat{\mathbf{y}}$ are unit vectors in the x- and y-directions, $\theta_i = k_0 z - \omega_0 t$ is the phase of the incident wave, k_0 is the incident wavenumber, $\omega_0 = ck_0$ is the frequency, and $\widehat{E}_{i0} = \mathrm{i}c\widehat{B}_{i0}$. For linearly polarized light with the electric field along the x-axis, we instead have $\mathbf{E}_{i0} = (\hat{\mathbf{x}}/2)\widehat{E}_{i0}\exp(\mathrm{i}\theta_i) + \text{c.c.}$, $\mathbf{B}_{i0} = (\hat{\mathbf{y}}/2)\widehat{B}_{i0}\exp(\mathrm{i}\theta_i) + \text{c.c.}$, and $\widehat{E}_{i0} = c\widehat{B}_{i0}$. We next assume small perturbations of the surface, so $\eta(x, y, t) = \eta_1(x, y, t)$, where $|\nabla||\eta_1| \ll 1$. (This implies small wave steepness $|\nabla\eta_1| \ll 1$ and that $|\eta_1\nabla| \ll 1$ when acting on $\mathbf{E}$ and $\mathbf{B}$.) Then $\mathbf{E}_{z=\eta} \approx \mathbf{E}_{0,z=0} + \mathbf{E}_{1,z=0} + \eta_1(\partial\mathbf{E}_0/\partial z)_{z=0}$ and $\mathbf{B}_{z=\eta} \approx \mathbf{B}_{0,z=0} + \mathbf{B}_{1,z=0} + \eta_1(\partial\mathbf{B}_0/\partial z)_{z=0}$, where $|\mathbf{E}_1| \ll |\mathbf{E}_0|$ and $|\mathbf{B}_1| \ll |\mathbf{B}_0|$. At $z = 0$, we have $\theta_i = \theta_0 = -\omega_0 t$. Writing $\mathbf{E}_r = \widetilde{\mathbf{E}}_r\mathrm{e}^{\mathrm{i}\theta_0}/2 + \text{c.c.}$ and $\mathbf{B}_r = \widetilde{\mathbf{B}}_r\mathrm{e}^{\mathrm{i}\theta_0}/2 + \text{c.c.}$, and linearizing the boundary conditions (11)–(13), we have, at $z = 0$,

$$\widetilde{B}_{rz1} - \widetilde{B}_{rx0}\frac{\partial\eta_1}{\partial x} - \widetilde{B}_{ry0}\frac{\partial\eta_1}{\partial y} = \widehat{B}_{i0}\left(\frac{\partial\eta_1}{\partial x} + \mathrm{i}\frac{\partial\eta_1}{\partial y}\right), \tag{16}$$

$$\widetilde{E}_{ry1} + \eta_1\frac{\partial\widetilde{E}_{ry0}}{\partial z} + \widetilde{B}_{rx0}\frac{\partial\eta_1}{\partial t} = \widehat{B}_{i0}\left(\mathrm{i}\omega_0\eta_1 - \frac{\partial\eta_1}{\partial t}\right), \tag{17}$$

and

$$\widetilde{E}_{rx1} + \eta_1\frac{\partial\widetilde{E}_{rx0}}{\partial z} - \widetilde{B}_{ry0}\frac{\partial\eta_1}{\partial t} = -\mathrm{i}\widehat{B}_{i0}\left(\mathrm{i}\omega_0\eta_1 - \frac{\partial\eta_1}{\partial t}\right). \tag{18}$$

To the zeroth-order, the boundary conditions at the foil surface $z = 0$ are that the electric field parallel to the foil is zero, $\mathbf{E}_0 = 0$, and therefore $\mathbf{E}_{r0} = -\mathbf{E}_{i0}$; and it follows from Maxwell's equations that $\mathbf{B}_{r0} = +\mathbf{B}_{i0}$ at $z = 0$. Since $\mathbf{E}_0 = 0$ and $\mathbf{B}_0 = 2\mathbf{B}_{i0}$ in equations (9) and (10), it is apparent that the foil is accelerated by the magnetic pressure of the EM field. The unidirectional wave equations $\partial\mathbf{E}_{r0}/\partial t - c\partial\mathbf{E}_{r0}/\partial z = 0$ and $\partial\mathbf{B}_{r0}/\partial t - c\partial\mathbf{B}_{r0}/\partial z = 0$ of the reflected wave have the boundary conditions $\mathbf{E}_{r0} = -(\hat{\mathbf{e}}/2)\widehat{E}_{i0}\mathrm{e}^{\mathrm{i}\theta_0(t)} + \text{c.c.}$, and $\mathbf{B}_{r0} = (\hat{\mathbf{e}}/2)\widehat{B}_{i0}\mathrm{e}^{\mathrm{i}\theta_0(t)} + \text{c.c.}$ at $z = 0$, with the solutions $\mathbf{E}_{r0} = -(\hat{\mathbf{e}}/2)\widehat{E}_{i0}\mathrm{e}^{\mathrm{i}\theta_0(t')} + \text{c.c.}$ and $\mathbf{B}_{r0} = (\hat{\mathbf{e}}/2)\widehat{B}_{i0}\mathrm{e}^{\mathrm{i}\theta_0(t')} + \text{c.c.}$, where the retarded time t' is obtained from $ct' = \xi$ with $\xi = z + ct$. It follows that $\widetilde{\mathbf{E}}_{r0} = -\hat{\mathbf{e}}\widehat{E}_{i0}\mathrm{e}^{\mathrm{i}\theta_0(t')-\mathrm{i}\theta_0(t)}$ and $\widetilde{\mathbf{B}}_{r0} = \hat{\mathbf{e}}\widehat{B}_{i0}\mathrm{e}^{\mathrm{i}\theta_0(t')-\mathrm{i}\theta_0(t)}$. Using $\partial t'/\partial z = 1/c$ and $\widehat{E}_{i0} = \mathrm{i}c\widehat{B}_{i0}$, we have $\widetilde{\mathbf{E}}_{r0}|_{z=0} = -\mathrm{i}\hat{\mathbf{e}}c\widehat{B}_{i0}$, $\widetilde{\mathbf{B}}_{r0}|_{z=0} = \hat{\mathbf{e}}\widehat{B}_{i0}$, $\partial\widetilde{\mathbf{E}}_{r0}/\partial z|_{z=0} = -\hat{\mathbf{e}}\omega_0\widehat{B}_{i0}$, and $\partial\widetilde{\mathbf{B}}_{r0}/\partial z|_{z=0} = -\mathrm{i}\hat{\mathbf{e}}k_0\widehat{B}_{i0}$, which is used in equations (16)–(18).

We assume a four-wave model in which the EM wave is scattered into two EM sidebands off the ripples in the foil surface so that $\widetilde{\mathbf{E}}_{r1} = \widehat{\mathbf{E}}_{r1+}\exp(-\mathrm{i}\omega t + \mathrm{i}k_x x + \mathrm{i}k_y y + \mathrm{i}k_{z+}z) + \widehat{\mathbf{E}}^*_{r1-}\exp(\mathrm{i}\omega^* t - \mathrm{i}k_x x - \mathrm{i}k_y y - \mathrm{i}k_{z-}{}^* z)$, $\widetilde{\mathbf{B}}_{r1} = \widehat{\mathbf{B}}_{r1+}\exp(-\mathrm{i}\omega t + \mathrm{i}k_x x + \mathrm{i}k_y y + \mathrm{i}k_{z+}z) + \widehat{\mathbf{B}}^*_{r1-}\exp(\mathrm{i}\omega^* t - \mathrm{i}k_x x - \mathrm{i}k_y y - \mathrm{i}k^*_{z-}z)$, and $\eta_1 = \hat{\eta}_1\exp(-\mathrm{i}\omega t + \mathrm{i}k_x x + \mathrm{i}k_y y) + \hat{\eta}_1^*\exp(\mathrm{i}\omega^* t - \mathrm{i}k_x x - \mathrm{i}k_y y)$. The vacuum wave equations for the scattered light, $\partial^2\mathbf{E}_{r1}/\partial t^2 - c^2\nabla^2\mathbf{E}_{r1} = 0$ and $\partial^2\mathbf{B}_{r1}/\partial t^2 - c^2\nabla^2\mathbf{B}_{r1} = 0$, then give the dispersion relation

$$\left(\pm\omega + ck_0\right)^2 - c^2\left(k_\perp^2 + k_{z\pm}^2\right) = 0, \tag{19}$$

where $k_\perp^2 = k_x^2 + k_y^2$. Equation (19) has the solutions $k_{z\pm} = \mp\sqrt{(k_0 \pm \omega/c)^2 - k_\perp^2}$, where the branches of the square root are chosen such that $\mathrm{imag}(k_{z\pm}) < 0$ for $\mathrm{imag}(\omega) > 0$. This gives radiating boundary conditions with waves propagating out from the foil and vanishing at $z = -\infty$, which is consistent with the model. For $k_0 > k_\perp$, the scattered wave is diffracted and propagates out from the foil at an angle φ to the negative z-axis, given by $\sin\varphi \approx k_\perp/k_0$, whereas for $k_0 < k_\perp$ the scattered wave is evanescent and decays rapidly with the distance from the foil. Separating wave modes proportional to $\exp(-\mathrm{i}\omega t + \mathrm{i}k_x x + \mathrm{i}k_y y)$ and $\exp(\mathrm{i}\omega^* t - \mathrm{i}k_x x - \mathrm{i}k_y y)$, the boundary conditions (16)–(18) yield the Fourier coefficients $\widehat{B}_{rz1+} = 2\widehat{B}_{i0}(\mathrm{i}k_x - k_y)\hat{\eta}_1$, $\widehat{B}_{rz1-} = 2\widehat{B}^*_{i0}(\mathrm{i}k_x + k_y)\hat{\eta}_1$, $\widehat{E}_{ry1+} = 2\mathrm{i}\widehat{B}_{i0}(\omega_0 + \omega)\hat{\eta}_1$, $\widehat{E}_{ry1-} = -2\mathrm{i}\widehat{B}^*_{i0}(\omega_0 - \omega)\hat{\eta}_1$, $\widehat{E}_{rx1+} = 2\widehat{B}_{i0}(\omega_0 + \omega)\hat{\eta}_1$, and $\widehat{E}_{rx1-} = 2\widehat{B}^*_{i0}(\omega_0 - \omega)\hat{\eta}_1$. From the divergence condition $\nabla\cdot\mathbf{E}_r = 0$ to the left of the foil, we obtain $\widehat{E}_{rz1+} = -2\widehat{B}_{i0}(\omega_0 + \omega)(k_x + \mathrm{i}k_y)\hat{\eta}_1/k_{z+}$ and $\widehat{E}_{rz1-} = -2\widehat{B}^*_{i0}(\omega_0 - \omega)(k_x - \mathrm{i}k_y)\hat{\eta}_1/k_{z-}$, and from the x- and y-components of Faraday's law $\partial\mathbf{B}_r/\partial t = -\nabla\times\mathbf{E}_r$, we have $\widehat{B}_{rx1+} = -2\mathrm{i}\widehat{B}_{i0}(k_y^2 + k_{z+}^2 - \mathrm{i}k_x k_y)\hat{\eta}_1/k_{z+}$, $\widehat{B}_{ry1+} = 2\widehat{B}_{i0}(k_x^2 + k_{z+}^2 + \mathrm{i}k_x k_y)\hat{\eta}_1/k_{z+}$, $\widehat{B}_{rx1-} = -2\mathrm{i}\widehat{B}^*_{i0}(k_y^2 + k_{z-}^2 + \mathrm{i}k_x k_y)\hat{\eta}_1/k_{z-}$, and $\widehat{B}_{ry1-} = -2\widehat{B}^*_{i0}(k_x^2 + k_{z-}^2 - \mathrm{i}k_x k_y)\hat{\eta}_1/k_{z-}$.

We next insert these results into equation (9) and separate terms proportional to exp $(-\mathrm{i}\omega t + \mathrm{i}k_x x + \mathrm{i}k_y y)$ and/or exp $(\mathrm{i}\omega^* t - \mathrm{i}k_x x - \mathrm{i}k_y y)$. This gives the dispersion relation for the RT-like instability for circularly polarized incident laser light,

$$\omega^4 - g_0^2 k_\perp^2 = \mathrm{i}\frac{\omega^2 g_0}{2}\sum_{+,-}\frac{k_\perp^2 + 2k_{z\pm}^2}{k_{z\pm}}, \tag{20}$$

where $k_{z\pm}$ is given by the solutions to equation (19), and $g_0 = F_0/M_0$. An analogous calculation for linearly polarized light with $\mathbf{E}_{i0} = (\hat{\mathbf{x}}/2)\widehat{E}_{i0}\exp(\mathrm{i}\theta_i) + \mathrm{c.c.}$, $\mathbf{B}_{i0} = (\hat{\mathbf{y}}/2)\widehat{B}_{i0}\exp(\mathrm{i}\theta_i) + \mathrm{c.c.}$, and $\widehat{E}_{i0} = c\widehat{B}_{i0}$ yields the dispersion relation

$$\omega^4 - g_0^2 k_\perp^2 = \mathrm{i}\omega^2 g_0\sum_{+,-}\frac{k_x^2 + k_{z\pm}^2}{k_{z\pm}}. \tag{21}$$

Equations (20) and (21) are the main results of this paper.

4. Discussion and numerical results

The dispersion relations (20) and (21) have one positive imaginary root $\omega = \mathrm{i}\omega_I$, which gives rise to a purely growing instability with growth rate ω_I. If the right-hand sides of equations (20) and (21) are neglected, we recover the standard RT instability with the growth rate $\omega_I = \sqrt{g_0 k_\perp}$. Two real-valued roots also exist which give rise to oscillatory solutions, similar to the case of the standard RT instability [1]. To compare with experiments and simulations, we note first that a critical dimensionless parameter of the system is the normalized acceleration $g_0/(c^2 k_0)$, which can be expressed in terms of commonly used laser–plasma parameters as $g_0/(c^2 k_0) = 2\sigma(Z_i m_e/m_i)(n_{cr}/n_e)a_0^2/(k_0 d)$, where Z_i is the charge state of the ions, m_e and m_i are the electron and ion mass, n_e/n_{cr} is the ratio of the electron density to the critical density, $a_0 = eE_{i0}/(m_e c\omega_0)$ is the normalized laser amplitude, d is the foil thickness, and the coefficient $\sigma = 1/2$ for linearly polarized light and $\sigma = 1$ for circularly polarized light. For example, Yan *et al* [3] used circularly polarized light ($\sigma = 1$) in their simulations to study the radiation pressure acceleration of a proton H^+ foil ($Z_i = 1, m_i = 1836 m_e$) with $n_0/n_{cr} = 10, k_0 d = 0.63$, and $a_0 = 5$, giving $g_0/(c^2 k) \approx 4.3 \times 10^{-3}$. On the other hand, Palmer *et al* [7] used linearly polarized light ($\sigma = 1/2$) in their experimental and simulation study of the RT instability of a carbon C^{6+} foil ($Z_i = 6, m_i \approx 12 \times 1836 \times m_e$) with $n_e/n_{cr} = 10^3$ and $k_0 d = 0.03$. Using their values $a_0 = 10$ and $a_0 = 20$ gives $g_0/(c^2 k) \approx 9.1 \times 10^{-4}$ and 3.6×10^{-3}, respectively.

Figure 1 shows the growth rates of the instability for a typical value $g_0/(c^2 k) = 3 \times 10^{-3}$. For the case of circularly polarized light, it is noticeable from figures 1(a) and (b) that the growth rate of the instability is close to that of the standard RT instability for $k_\perp < k_0$, has a sharply peaked maximum at $k_\perp \approx k_0$, and has a lower growth rate than the standard RT instability for $k_\perp \gtrsim 1.5 k_0$. For linearly polarized light, we see in figures 1(c) and (d) that the instability is strongly anisotropic, with a larger growth rate for perturbation wavenumbers in the x-direction, parallel to the electric field and perpendicular to the magnetic field of the incident EM wave. This may be because it is energetically easier to move and rearrange than to bend magnetic field lines. Similar situations often occur in plasmas confined by a non-oscillatory magnetic field and give rise to RT-like instabilities, such as the gravitational and flute instabilities [20], where the perturbation wavenumbers of the fastest-growing unstable waves are at angles almost perpendicular to the magnetic field. Recent experiments and simulations [7] show that the RT instability gives rise to structures with wavelengths about the same as the laser wavelength, which is consistent with figure 1 and is attributed to laser diffraction effects [7]. On the other hand, the numerical simulations in [16] revealed that in the case of P-polarization, strong electron heating occurred and the surface rippling can be 'washed out' by the quiver motion of the electrons, which might diminish the importance of the instability. As seen in figure 1, the RT-like instability has also a large growth rate for $k_\perp \gg k_0$, where the instability can be expected to saturate nonlinearly by forming small-scale structures but without disrupting the foil. The most severe instability is at $k_\perp \approx k_0$, which leads to the disruption of the foil and to the broadening of the energy spectrum [6]. We notice that in [16] an infinite growth rate is predicted when the perturbation wavenumber in the foil equals the laser wavenumber. This is due to the assumption of space and time harmonic scattered electromagnetic field (see their equations (1) and (2)), leading to the excitation of a resonant standing surface wave. Taking into account the exponential growth in time of the scattered wave due to the RT-like instability avoids the singularity, and the growth rate becomes well defined when the perturbation wavenumber in the foil equals the laser wavenumber. A scheme tailored to reduce the maximum of the growth rate at $k_\perp \approx k_0$ of the RT-like instability may potentially make laser-driven radiation pressure acceleration schemes more tractable.

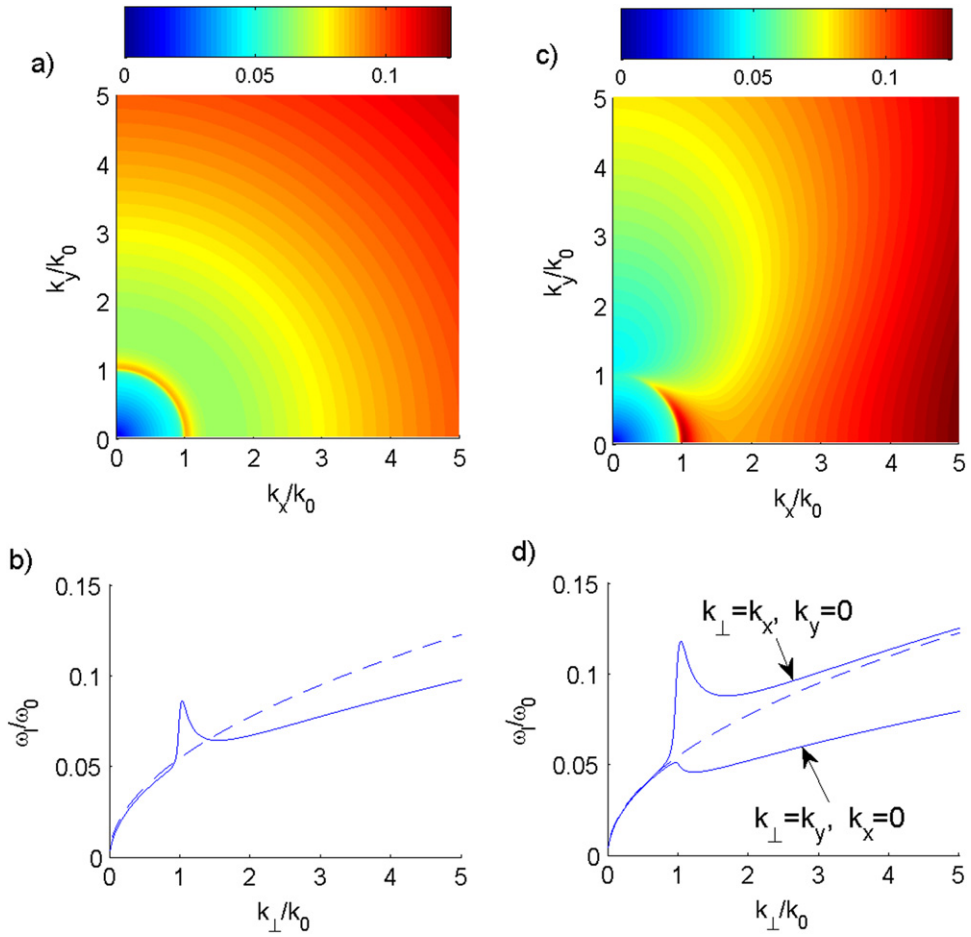

Figure 1. The normalized growth rate ω_I/ω_0 of the instability for (a), (b) circularly polarized waves as obtained from equation (20) and (c), (d) linearly polarized waves as obtained from equation (21). (a), (c) Color plots of the growth rate as a function of $(k_x/k_0, k_y/k_0)$. (b), (d) Line plots of the growth rate (solid lines). A comparison is made with the standard Rayleigh–Taylor instability (dashed line).

Acknowledgments

Useful discussions with C S Liu, X. Shao and TC Liu at the University of Maryland; Z-M Sheng, T Heelis, and A W Cross at the University of Strathclyde; and F Pegoraro at the University of Pisa are gratefully acknowledged. This work was supported by the Engineering and Physical sciences Research Council (EPSRC), UK, grant no. EP/M009386/1.

References

[1] Ott E 1972 Nonlinear evolution of the Rayleigh-Taylor instability of a thin layer *Phys. Rev. Lett.* **29** 1429
[2] Pegoraro F and Bulanov S V 2007 Photon bubbles and ion acceleration in a plasma dominated by the radiation pressure of an electromagnetic pulse *Phys. Rev. Lett.* **99** 065002
[3] Yan X Q, Lin C, Sheng Z M, Guo Z Y, Liu B C, Lu Y R, Fang J X and Chen J E 2008 Generating high-current monoenergetic proton beams by a circularly polarized laser pulse in the phase-stable acceleration regime *Phys. Rev. Lett.* **100** 135003
[4] Chen M, Pukhov A, Sheng Z M and Yan X Q 2008 Laser mode effects on the ion acceleration during circularly polarized laser pulse interaction with foil targets *Phys. Plasmas* **15** 113103
[5] Robinson A P L, Zepf M, Kar S, Evans R G and Bellei C 2008 Radiation pressure acceleration of thin foils with circularly polarized laser pulses *New J. Phys.* **10** 013021
[6] Liu T-C, Shao X, Liu C-S, Su J-J, Eliasson B, Tripathi V, Dudnikova G and Sagdeev R Z 2011 Energetics and energy scaling of quasi-monoenergetic protons in laser radiation pressure acceleration *Phys. Plasmas* **18** 123105
[7] Palmer C A J *et al* 2012 Rayleigh-Taylor instability of an ultrathin foil accelerated by the radiation pressure of an intense laser *Phys. Rev. Lett.* **108** 225002
[8] Adusumilli K, Goyal D and Tripathi V K 2012 Radiation pressure acceleration of corrugated thin foils by Gaussian and super-Gaussian beams *Phys. Plasmas* **19** 013102
[9] Smalyuk V A 2012 Experimental techniques for measuring Rayleigh-Taylor instability in inertial confinement fusion *Phys. Scr.* **86** 058204

[10] Wu D, Zheng C Y, Qiao B, Zhou C T, Yan X Q, Yu M Y and He X T 2014 Suppression of transverse ablative Rayleigh-Taylor-like instability in the hole-boring radiation pressure acceleration by using elliptically polarized laser pulses *Phys. Rev.* E **90** 023101
[11] Khudik V, Yi S A, Siemon C and Shvets G 2014 The analytic model of a laser-accelerated plasma target and its stability *Phys. Plasmas* **21** 013110
[12] Rayleigh L 1882 Investigation of the character of the equilibrium of an incompressible heavy fuid of variable density *Proc. London Math. Soc.* **14** 170
[13] Taylor G I 1950 The instability of liquid surfaces when accelerated in a direction perpendicular to their planes *Proc. R. Soc. London Ser.* A **201** 192
[14] Gamaly E G 1993 Instability of the overdense plasma boundary induced by the action of a powerful photon beam *Phys. Rev.* E **48** 2924
[15] Macchi A, Cornolti F and Pegoraro F 2002 Two-surface wave decay *Phys. Plasmas* **9** 1704
[16] Sgattoni A, Sinigardi S, Fedeli L, Pegoraro F and Macchi A 2015 Laser-driven Rayleigh-Taylor instability: plasmonics effects and three-dimensional structures *Phys. Rev.* E **91** 013106
[17] Lindgren T, Stenflo L, Kostov N and Zhelyazkov I 1985 Three-wave interaction in a cold plasma column *J. Plasma Phys.* **34** 427
[18] Stix T H 1992 *Waves in Plasmas* (New York: American Institute of Physics)
[19] Jackson J D 1999 *Classical Electrodynamics* 3rd ed (New York: Wiley)
[20] Goldston R J and Rutherford P H 1997 *Introduction to Plasma Physics* (Philadelphia: Institute of Physics Publishing)